Environ. Eng. Res. Vol. 9, No. 4, pp. 143~153, 2004
Korean Society of Environmental Engineers

DEVOLATILIZATION OF SOLID WASTE PARTICLES AND COMBUSTION OF VOLATILES IN A FLUIDIZED BED: MODELING AND EXPERIMENTAL VALIDATION

Jinhwan Choi and Sangmin Choi†

Department of Mechanical Engineering
Korea Advanced Institute of Science and Technology
Yusong-Gu, Daejon, 305-701, Korea
(received April 2003, accepted July 2004)

Abstract : Devolatilization and char combustion of solid fuel particles of which typical size was in the order of 2cm and combustion of evolved volatiles were investigated, using two different FBCs (fluidized bed combustors). By varying the combustion conditions, fraction of bunt carbon was estimated from gaseous concentration measurements in a laboratory-scale FBC and the fraction of the original volatiles burnt above the bed was determined from the calorimetric calculation in a semi-pilot-scale FBC.

Combustion of solid particle and volatiles in a FBC was modeled by a simulation model where two sub models were introduced; a particle combustion model and a three-phase bed model. The particle combustion model considered devolatilization and char combustion, external and internal heat and mass transfer, and changing fuel properties. The three phase mathematical model for a fluidized bed described the bed hydrodynamics and gas exchange between phases as well as the combustion of volatiles from the fuel particle. The particle combustion model provided the inlet conditions for the fluidized bed model such as gaseous products and the fluidized bed model provided the combustion environment for the particle combustion model.

Comparison of the experimental results and the predicted results by the model showed a good agreement as to the fraction of carbon conversion and the fraction of volatiles burnt in the freeboard. Interrelation of the fluidized bed conditions and particle combustion was adequately treated in this simulation model by combining the particle combustion model and the fluidized bed model.

Key Words : devolatilization, char combustion, fluidized bed combustor, particle combustion model, three phase bed model

INTRODUCTION

Fluidized bed combustors (FBCs) can burn a wide range of solid fuels, such as coal, solid wastes including sludges with a high percentage of moisture and ash, and the highly volatile biomass and RDF, thanks to the good mixing and long residence time.[1~4)]

Growing interest in the application of FBC technology to high-volatile fuels is emphasizing the importance of understanding the sub-processes, such as devolatilization, volatile mixing and combustion.[5)] These processes are closely interrelated with the achievement of substantially higher combustion efficiency and uniform temperature profiles in the combustor, which would ultimately lead to lower level of pollution.

† Corresponding author
E-mail: smchoi@mail.kaist.ac.kr
Tel: +82-42-869-3030, Fax: +82-42-862-1284

FBC design parameters should be optimized to guarantee low pollution and high combustion efficiency. One of the most important factors in operating FBC is to maintain uniform temperature distribution both in the bed and in the freeboard. In order to control the temperature distribution, the amount of heat release should be optimized.[6] It is not possible without precise information on fuels in FBC.

As to the devolatilization and combustion of the volatiles, three assumptions were suggested: (1) the volatiles are released and burned instantaneously at the feed point[7~9]; (2) uniform volatiles combustion throughout the bed[10]; and (3) volatiles burning mainly in the freeboard by forming a plume.[11,12] Validity of these assumptions depends on the comparative rates of devolatilization and their subsequent combustion in comparison with the rates of solid mixing and gaseous mixing in the bed. The mixing time lies within 10 sec[10], but the devolatilization time ranges from a few to hundreds of seconds, according to the experimental condition: bed temperature, particle size, fuel type, etc.[13~17]

In this study, the combustion processes of solid particles, of which combustible is mostly volatile matters, were characterized through experimental and numerical approaches. The fuel particle in the fluidizing bed was numerically modeled using the concept of a dynamic model suggested by Winter et al.[14] who considered a temperature profile inside a particle, rather than assuming an isothermal particle. The gas phase mixing and reaction of volatiles in isothermal fluidized beds was explained based on the three-phase model. The nonisothermality of the bed resulting from the combustion reactions is taken into account through inclusion of an energy balance for the bubble phase as Sriramulu et al. did.[18] This paper reports an attempt to develop acombined simulation of the particle combustion model and the fluidized bed model that considers the interrelation between fuel particles and the fluidized bed system. The particle combustion model provides the inlet conditions for the fluidized bed model such as gaseous product and the fluidized bed model provides the combustion environment for the particle combustion model.

EXPERIMNETAL

Two experimental apparatuses were constructed to generate the combustion environment similar to the one in an actual FBC as shown in Figure 1. The main bodies of FBCs were made of stainless tubes and were covered with rock-wool blanket of low thermal conductivity. External electrical heaters were used to heat the combustor body and fluidizing gas, hence providing a uniform combustor temperature.

Laboratory Scale FBC (batch operation)

Combustion characteristics of the fuel particle were investigated in a laboratory scale FBC. A batch of fuel particles was introduced into the bed from the top of the combustor. The composition of the combustion gas was continuously measured at the outlet. The progress of reaction was observed by determining the fraction of carbon conversion (f), which was determined from the measured concentration of carbon containing species, namely CO, CO_2 and C_xH_y. The accuracy of the experiment was checked with the carbon recovery (r_c). The definitions of the experimental parameters are as follow.

$$f = \frac{n}{N} \times 100, \quad where$$
$$n = \int_0^t Q(C_{CO} + C_{CO_2} + C_{C_xH_y})dt, \qquad (1)$$
$$N = \int_0^{t_n} Q(C_{CO} + C_{CO_2} + C_{C_xH_y})dt$$

$$r_C = \frac{N}{carbon\ in\ fuel} \times 100, \quad where$$
$$carbon\ in\ fuel = \frac{f_c \times m_{fuel}}{12} \qquad (2)$$

Some features of this experimental methodology were adopted from the coal combustion experiments by Lau et al..[1,18]

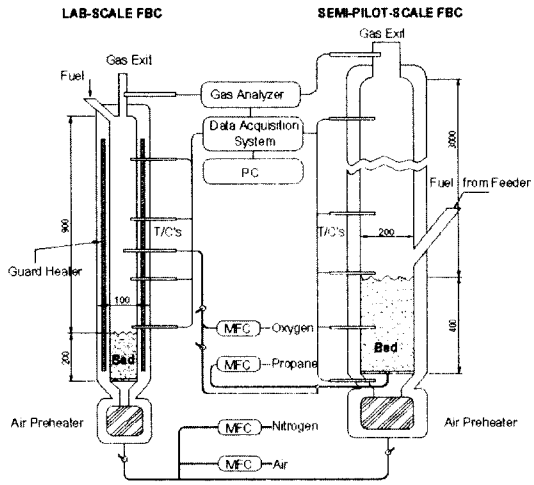

Figure 1. Fluidized bed combustors.

Semi-pilot-scale FBC (continuous operation)

The semi-pilot-scale FBC was run continuously and temperature profile in the combustor and gas concentration at the exit were measured under the steady state condition. Percent of excess air was adjusted by changing the feeding rate of the fuel and by adding nitrogen to the fluidization air. An indirect method, energy balances in conjunction with mass balances, was adopted to determine the extent of combustion of volatiles in the freeboard where it is difficult to measure the gas concentration. Bautista-Margulis et al.[19] used the similar method for the combustion of coal volatiles.[20,21]

The energy balances were performed in the bed and six freeboard sections divided by the temperature measuring positions. In the bed section, the heat inputs were the enthalpy of the fluidizing gas and the fuel, the gross calorific value of the fuel. The heat output were the enthalpy of combustion gas, heat loss to surroundings, and heat release to the freeboard by unburned combustibles. The energy balance equation could be constructed as follow.

$$\dot{Q}_{vf} = (\dot{Q}_f + \dot{Q}_{fuel} + \dot{Q}_{g\_in}) - (\dot{Q}_{g\_out} + \dot{Q}_{b\_loss}) \quad (3)$$

Therefore the energy fraction of the volatile component transferred into the freeboard and burnt there was deduced from the overall energy balance.

$$\Delta_{vf} = \frac{\dot{Q}_{vf}}{\dot{Q}_{vf\_total}}, \; where \;\; \dot{Q}_{vf\_total} = \dot{m}\left(LHV_{fuel} - HHV_{char} \times f_{char}\right) \quad (4)$$

At a freeboard section, the energy balance equation and the energy fraction could be made as follows;

$$\dot{Q}_{vf\_i} = \dot{Q}_{g\_in\_i} - (\dot{Q}_{g\_out\_i} + \dot{Q}_{loss\_i}), \; therefore \;\; \Delta_{vf\_total} = \sum_i \frac{\dot{Q}_{vf\_i}}{\dot{Q}_{vf\_total}} \quad (5)$$

PARTICLE COMBUSTION MODEL AND FLUIDIZED BED MODEL

Figure 2 shows the flow chart of the model constructed by combining a particle combustion model and a fluidized bed model. The model for thefuel particle combustion model predict the progress of combustion of the particle and predicts the amount of gaseousmatters from the burning particle, which are introduced into the fluidized bed model as the inlet conditions. The fluidized bed model solves the gas phase mixing and reaction of volatiles in the bed, subsequently provides the changed conditions of the particle combustion to the particle model.

The gaseous matters generated from the particle are assumed to distribute uniformly in the cloud-wake and emulsion phases in the three-phase fluidized bed model.

Particle Combustion Model

The fuel particles are divided into many homogeneous spherical shells. Each spherical-shell experiences one-dimensionally progressing combustion processes; drying, devolatilization, and char combustion. At each time step, energy equation was solved for each shell by taking into account convective and radiant heat transfer to the particle and heat transfer inside the particle by conduction. The evaporation and devolatilization model was solved according to the temperature of each shell. Thermal decompo-

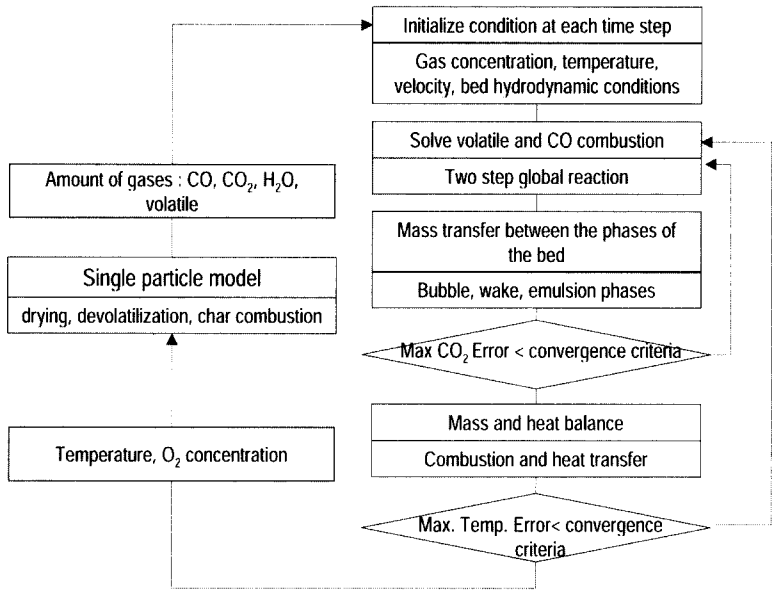

Figure 2. Flow-chart describing the calculation process in the fluidized bed model combined with a particle combustion model.

sition heat and latent heat for evaporation were considered in the energy equation as well as the enthalpy loss by mass transfer of the vaporproducts from the drying and the devolatilization processes. The char combustion was modeled by using the concept of shrink particle model and considered to take place at the outer shell after all the moisture and volatiles were released.

The model assumes the particle to be an unsteady one-dimensional system. The energy conservation equation and the corresponding boundary condition become:

$$\frac{\partial}{\partial t}(\rho\, c_p T) = \frac{1}{r^2}\frac{\partial}{\partial r}\left(r^2 k \frac{\partial T}{\partial r}\right) - \frac{1}{r^2}\frac{\partial}{\partial r}(r^2 \rho_g U_g c_g T) - q_{reaction} \quad (6)$$

$$\left.\frac{\partial T}{\partial r}\right|_{r=0} = 0, \quad \left. k\frac{\partial T}{\partial r}\right|_{r=R} = h_{eff}(T_b - T_s)$$

$$(boundary\ condition),\ T_0 = 293K(initial\ condition) \quad (7)$$

where U_g is the velocity of vapors inside the particle. In this model, U_g is assumed to be very high, which means the volatile or water-vapors are discharged outside the particle immediately after they generated. The last term of the energy equation ($q_{reaction}$) represents the heat generation and consumption by reaction such as char combustion, evaporation and devolatilization.

Sub-models for the heat and mass transfer, the char combustion and the devolatilization were given in Table 1, in addition to a method of the property calculation changed by reaction. The fragmentation and attrition increase the reaction rate of the char by enlarging the volumetric surface area by generating fine fragments of low heat capacity and large volumetric surface area. There's no appropriate way except some ambiguousones to reflect the phenomena. To take into account the fragmentation and attrition effects to the reaction rate, a modified model was suggested as shown in Table 1. The attrition effect constant was introduced from the drastic simplifying hypothesis; the chemical reaction rate was boosted up by the some fraction of the mass transfer rate.

Table 2 reports the values of the main physical parameters utilized in the present simulation, which are typical for the wood particle.

Fluidized Bed Model

Table 1. Sub-models for heat and mass transfer, char combustion and devolatilization

Mass transfer	$Sh = 2\varepsilon + 0.69\left(\frac{\mathrm{Re}}{\varepsilon}\right)^{0.5} Sc^{0.33}$	Devolatiliza-tion	$\frac{dX_{volat}}{dt} = -A\exp\left(-\frac{E}{RT}\right)X_{volat}$, $A:5.3\times10^4, E:8.53\times10^4$	[22]
Heat transfer	$\frac{hl_l}{k_g} = \frac{0.125(1-\varepsilon_{mf})\left[1+33.3\left[\left(\frac{u-u_{mf}}{u_{mf}}\right)^{1/3}\left(\frac{\rho_p c_p}{k_g g}\right)^{1/3}(u-u_{mf})\right]^{-1}\right]^{-1}}{1+\frac{k_g}{2c_p\mu}\left[1+0.28(1-\varepsilon_{mf})^2\left(\frac{\rho_g}{\rho_p-\rho_g}\right)^{0.5}\left[\left(\frac{\rho_g c_p}{k_g g}\right)^{1/3}(u-u_{mf})\right]^2\frac{u_{mf}}{u-u_{mf}}\right]}$ $+0.165\,\mathrm{Pr}^{1/3}\left(\frac{\rho_g}{\rho_p-\rho_g}\right)^{1/3}\left[1+0.05\left(\frac{u-u_{mf}}{u_{mf}}\right)^{-1}\right]^{-1}+\frac{d_s\omega\sigma}{k_g}\left(\frac{T_b^4-T_s^4}{T_b-T_s}\right)$ Where $l_l=\left[\frac{\mu}{\sqrt{g(\rho_p-\rho_g)}}\right]^{2/3}$, $\sigma = 5.67\times10^{-8}$			[23]
Char combustion	$\frac{dM_{char}}{dt} = -W_{char}A_{eff}C_{O_2}\frac{1}{1/(\eta k_r + k_{attrition}) + 1/k_m}$, $k_r = 2.3T\exp(-1110/T)$ $k_{attrition} = Char_{attrition}$ effect on reaction rate $= \eta k_m$ where $\Theta=\frac{2(\alpha+\beta)}{(\alpha+2\beta)}$, $(\alpha+\beta)C+\left(\frac{\alpha}{2}+\beta\right)O_2\rightarrow\alpha CO_2+\beta CO$ $\frac{\alpha}{\beta}=1336\exp(-7463/T)$ [for $T<970K$] $=0.00472\exp(4539/T)$ [for $970<T<1220K$]				[24]
Fuel properties	$k=\frac{\sum_i X_{-i}k_i}{\sum_i X_{-i}}+13.5\sigma T^3\frac{d}{\omega}$, d :pore diameter 0.01mm, w solids emissivity 0.95 $c=\frac{\sum_i X_{-i}c_{P-i}}{\sum_i X_{-i}}$, $\rho=\rho_0\sum_i X_{-i}$, $X_{-i}=\frac{M_{-i}}{total\_M_0}$ where $total\_M_0$:initial total mass				

Table 2. Main physical parameters utilized in the present simulations

Parameter	Symb.	Value	Units	Parameter	Symb.	Value	Units
Conductivity	k_v	0.21	W/m^{2}K	Specific heat	c_v	2000	J/kgK
	k_c	0.085			c_c	1000	
	k_a	0.1			c_a	1000	
Mass fraction	X_v	0.8		Heat of devolatilization	q	-480	J/kg
	X_c	0.19		Char attrition constant	ϕ	0.9	
	X_a	0.01		Density	ρ_0	600	kg/m^3

In the three-phase bed model, the fluidized bed is assumed to consist of three distinct phases namely, a solid free bubble phase, a cloud-wake phase, and an emulsion phase.[19] The kinetic rate parameters, the correlations for the estimation of the bed hydrodynamic parameters, and governing equations are summarized in Table 3.

The particulate phases are assumed to be isothermal because the temperaturechange in the phases is negligible in the steady state due to the high specific heat of inert particles.

EXPERIMENTAL RESULTS AND MODEL PREDICTIONS

Internal temperature of the particle

An accurate estimate of the particle temperatureis essential to evaluate the mechanisms of the drying and devolatilization, and to predict the reaction rate of char combustion.

Temperature at the center of awood particle was measured with a 0.3mm thermocouple spiked into the particle. Figure 3 shows modeling and experimental results of the particle progress of temperaturevarying the moisture

Table 3. Sub-models for heat and mass transfer, char combustion and devolatilization

Parameter and correlation	$d_B = \left[0.46\frac{(u-U_{mf})^{0.5}z}{g^{0.25}} + d_{B,init}^{1.25}\right]^{4/5}$ $d_{B,init} = 1.3(u-U_{mf})^{0.4} N_{or}^{-0.4} g^{-0.2}$ $U_B = (u-U_{mf}) + 0.71\sqrt{gd_B}$ $f_W = 0.3$	Gas exchange coefficient	$K_{BW} = 4.5\left(\frac{U_{mf}}{d_B}\right) + 5.87\left(\frac{D_g^{0.5} g^{0.25}}{d_B^{1.25}}\right)$ $K_{WE} = 6.77\left(\frac{D_g \varepsilon_{mf} U_{Br}}{d_B^3}\right)^{1/2}$ with $U_{Br} = 0.71\sqrt{gd_B}$	[25, 26]
Material balance equation	$u = U_B f_B + f_B(f_W)\varepsilon_{mf} U_B + [1 - f_B(1+f_W)]\varepsilon_{mf} U_E$, $U_E = U_{mf}/\varepsilon_{mf}$ **Bubble phase** $f_B \frac{\partial C_{i,B}}{\partial t} + \frac{\partial (U_B f_B C_{i,B})}{\partial z} + f_B K_{BW}(C_{i,B} - C_{i,W}) + \dot{m}_{i,B} = 0$ **Wake-cloud phase** $f_B f_W \varepsilon_{mf} \frac{\partial C_{i,W}}{\partial t} + \varepsilon_{mf} \frac{\partial (U_W f_B f_W C_{i,W})}{\partial z} + f_B f_W \varepsilon_{mf} K_{BW}(C_{i,W} - C_{i,B}) + f_B f_W \varepsilon_{mf} K_{EW}(C_{i,W} - C_{i,E}) + \dot{m}_{i,W} = 0$ **Emulsion phase** $(1 - f_B - f_B f_W)\varepsilon_{mf} \frac{\partial C_{i,E}}{\partial t} + \varepsilon_{mf} \frac{\partial (U_E(1 - f_B - f_B f_W) C_{i,E})}{\partial z} + \varepsilon_{mf}(1 - f_B - f_B f_W) K_{EW}(C_{i,E} - C_{i,W}) + \dot{m}_{i,E} = 0$			[18]
Energy Eq. in bubble phase	$\frac{\partial (c_{g,B} f_B \rho_{g,B} T_{g,B})}{\partial t} + \frac{\partial (c_{g,B} U_B f_B \rho_{g,B} T_{g,B})}{\partial z} + f_B \sum_i \Delta H_{i,B} rate_{i,B} + 6\frac{h_B}{d_B} f_B (T_{g,B} - T_{bed}) = 0$ $h_B = 0.25 U_B \gamma_B c_p \rho_p \left[1 - \exp\left(\frac{-6h_{Br}\tau}{c_p \rho_p d_p}\right)\right]$, $\frac{h_{Br} d_p}{k_g} = 2 + 0.6\,\mathrm{Re}_p^{1/2}\,\mathrm{Pr}_p^{1/3}$, $\tau = \sqrt{1.14 d_B / g}$, $\gamma_B = 1.5 \times 10^{-3}$			[27]

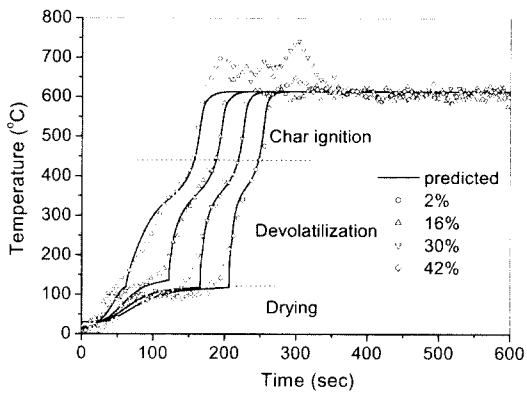

Figure 3. Temperature-profile for the wood at the center (d_p=2.5cm, T_b=600°C, u=0.77m/sec, moisture content = 0 ~ 42%).

content. The time-resolved temperature profile shows the reaction at the center of the particle; the drying period in which the particle temperature rises very slowly near and below 100°C, the char combustion period started where the temperaturerise very rapidly about 500°C and the devolatilization period between the two periods. After sharp rise during the initial phases of char combustion, temperature maintains at a constant level during the char combustion.

At the end of the devolatilization the wood particle started to crack from the point of inserted thermocouple. Oxygen diffused through the crack enabled the char combustion, which resulted in the temperature peaks. The irregularity of the crack led to inconsistent values of the temperature peak. When the crack grew enough, the thermocouple was separated from the particle. The temperature of the later part of the peak was not the particle temperature, but the bed temperature instead.

Parametric Study

Figure 4(a) shows experimental and modeling results for the dry wood particle of different size. Rate of carbon conversion duringthe devolatilization phase decreased with the sizes of particles. The trend was maintained during the char combustion.

As shown in Figure 3, during the drying period, the particle temperature rises very slowly. At the low temperature devolatilization goes on slowly even though it starts at the same time as the drying. In spite of the longer devolatilization time, the overall combustion time does not increase greatly (see Figure 4 (b)), which means that char combustion has gone

independently to other two processes. Overlap of the processes becomesmore significant when the moisture content gets higher; the char combustion is going on in the dry outer shell of the fuel particle, which has been already devolatilized while the inner shell is under devolatilization period.

Figure 4(c) and (d) show the results obtained for the wood particle in varying operating conditions; bed temperature, oxygen concentration of fluidizing gas. Higher temperature increased the rates of the devolatilization and char combustion and led to shorter combustion times.

The fraction of carbon conversion profiles of Figure 4(d) for wood particles suggested that the oxygen concentration of the fluidizing gas had little effect on the devolatilization. But they changed the rate of char combustion for which oxygen was necessary. The higher oxygen concentration guaranteed higher mass transfer rate of oxygen at the char particle's surface, which led to higher char combustion rates.

Values of the carbon recovery were over 90% for all cases, which meant that most fuel carbon injected to the combustor was converted into the gas phase carbon (CO, CO_2 and C_xH_y) and recovered by the gas analyzing system. The validity of this experimental methodology could be verified with the high value of the carbon recovery.

Combustion of Volatiles for the Wood

Figure 5 shows the extent of volatile combustion above the bed for the wood, which was calculated from the simulation model and the energy balance in the bed and the freeboard of the semi-pilot-scale FBC. The fractions were found to range from 5 to 35% with excess air levels varying from 65 to 15% and at the bed

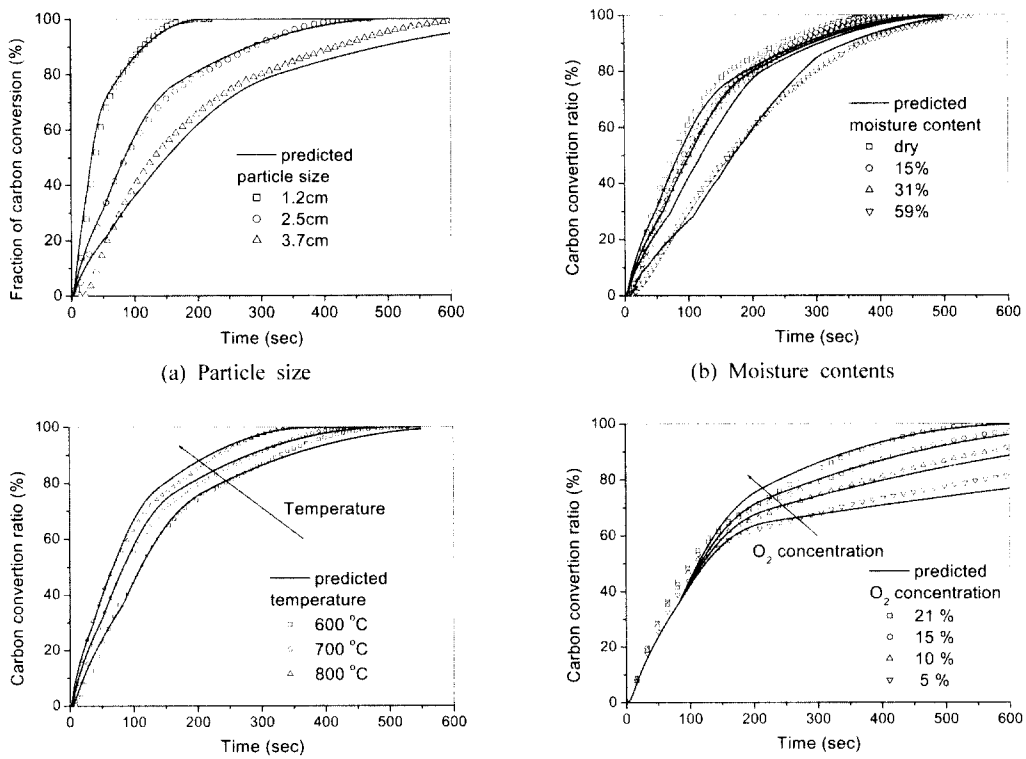

(a) Particle size

(b) Moisture contents

(c) Bed temperature

(d) Oxygen concentration

Figure 4. Comparisons of predicted and experimentally measured fraction of carbon conversion for T_b = 600 ~ 800°C, u=0.86m/sec, CO_2 5 ~ 21%, moisture contents 0 ~ 59%, d_p 1.2 ~ 3.7cm.

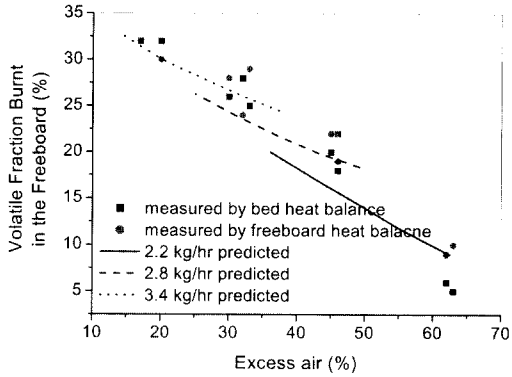

Figure 5. Theoretical and experimental comparison of the combustion of wood volatiles: constant flow rate, varying oxygen concentration of the fluidized air to adjust excess air.

temperature of 850 ~ 980°C. Values of fraction estimated from the energy balance in the freeboard showed more scattercompared to the valuesfrom the energy balance in the bed. In the freeboard, heat loss was comparable to the total amount of heat release, which was the main source of error.

The model results are consistent with the experimental results. The model results reflect the effects of varying fuel feed rate, which is hidden in the experimental results due to the error. On the same excess air, the extent of volatiles combustion above the bed increases when the fuel feed rate increases. Figure 6 shows the gas concentration in the emulsion phase and the bubble phase at the same excess air of 37%. The temperature values used in the model are the measured values. As feed rate increases the oxygen lack region starts in the lower part in the emulsion phase (see Figure 6 (a)), hence incomplete combustion product such as CO and volatiles increase in the region (see Figure 6 (b)). The bed temperature varies as the feed rate changes, but the effects of the temperature is small compared with that of excess air.

CONCLUSION

A dynamic simulation model which simulates the behavior of a single fuel particle was proposed to describe the processes of fuel particle combustion in the FBC. In spite of the drastically simplified assumptions, the simulation showed a good agreement with the experimental results for various cases of moisture content, particle sizes, bed temperature and oxygen concentration of the fluidizing gas. The present simulation model gave a picture of the mechanisms of combustion for the large fuel particle with high volatile content in the FBC. The drying, devolatilization and char combustion processes overlapped with each other. Temperature profile of the particle was very important in drying and devolatilization, which took place at relatively lower particle temperatures. The char

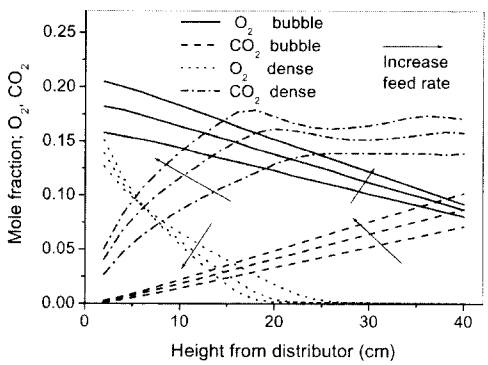

(a) O_2, CO_2 fraction

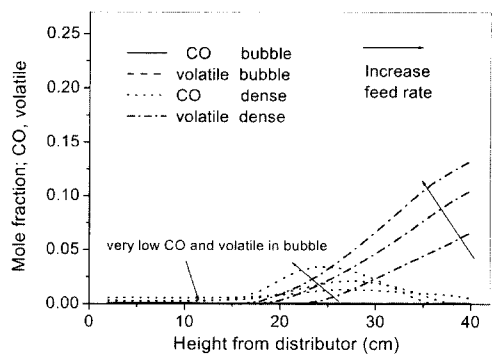

(b) CO, volatile fraction

Figure 6. Gas fraction with varying fuel feed rate: dry wood, T_b 825, 915, 968°C, feed rate 2.2, 2.8, 3.4 kg/hr, excess air 37%

NOTATION

A_{eff}	effective surface area	m^2
$C_{<subscript>}$	concentration <CO>: CO , <CO_2>: CO_2, <C_xH_y>: hydro carbon	mol/Nm^3
$c_{<subscript>}$	heat capacity, <P>:fuel particle, <g>gas, <p>fluidized particle, <c> char, <v>: volatile, <a>: ash	W s /kgK
D_g	diffusivity	m^2/sec
d	pore diameter	m
d_B	bubble diameter	m
f	fraction of carbon conversion	%
$f_{<subscript>}$	<C>: carbon mass fraction from element analysis <char>: char mass fraction, <W> wake fraction of bubble	
g	acceleration due to gravity	m/s^2
h_{eff}	effective heat transfer coefficient	W/ m^2K
HHV	higher heating value	J/kg
$K_{<subscript>}$	gas exchange coefficient, <BW>: between bubble and wake, <WE>: between wake and emulsion, <BE>: between bubble and emulsion	1/sec
k	thermal conductivity	W/m^2K
$k_{<subscript>}$	<r>: reaction rate, <m>: mass transfer rate,<attrition>: reaction rate by attrition effect, <g>: gas thermal conductivity	m/sec
$LHV_{<subscript>}$	gross calorific value, <fuel>: fuel, <char>: char	J/kg
$l_{<subscript>}$	characteristic length scale <l>: laminar flow	m
m_{fuel}	mass of fuel particle	kg
$\dot{m}$	fuel feed rate	kg/sec
$\dot{m}_{<subscrip>}$	mass generation by reaction , <B>: bubble, <E>:emulsion, <W>: wake	kg/sec
MFC	mass flow controller.	
m_{fuel}	mass of fuel input	G
N	total mole number	mol
n	mole number	mol
Pr	Prandtl number	
Q	combustion gas flow rate	Nm^3/sec
$\dot{Q}_{<subscript>}$	enthalpy, <b_loss>: bed heat loss, <fuel>: enthalpy of fuel, <g_in>: enthalpy of fluidization gas, <g_out>: enthalpy of combustion gas, <vf>: total heat of volatile transfer to freeboard,	W
R	gas constant, correlation coefficient in linear fitting	J/molK
Re	Renold number	
r	radius	m
r_c	carbon recovery	%
Sh	Sherwood number	
Sc	Schmidt number	
$T_{<subscript>}$	temperature, <g>: gas, <0>: initial <b>: bed	°C
t	time	sec
t_B	overall burnout time	sec
T/C	thermo couple	
u	superficial velocity	m/sec
$U_{<subscript>}$	gas velocity, <mf> minimum fluidization velocity, <g>: gas, <B>: bubble phase, <E>: emulsion or particulate phase	m/sec
$X_{<subscript>}$	mass fraction, <c>: char, <v>: volatile, <a>: ash, <CO>:CO mole fraction, <CO_2>: CO_2 mole fraction	
$\rho_{<subscript>}$	density, <0>:initial value, <g>: gas, <p>: fluidize bed particle	kg/m^3
Δ_{vf}	energy fraction of the volatile transferred into the freeboard	%
σ	Boltzman constant	
ε	void fraction	
ε_{mf}	void fraction at minimum fluidization	
μ	viscosity	kg/ms
ϕ	attrition constant	
Θ	gravimetric stoichiometric constant	
ω	emissivity	

combustion was accompanied by rapid increase in temperature and was going on at a constant level of intra-particle temperature.

Fraction of the volatiles burnt in the freeboard was experimentally determinedby applying the calorimetric method. The fractions were found to range from 5 to 35%. The amount of volatiles-burnt in the freeboard was linearly dependanton the excess air ratio, for the temperature ranges of the test, i.e., between 870°C and 950°C, which meant the mixing of volatiles and oxygen in the bed was the main parameter of the volatile combustion. The fluidized bed model combined with the particle combustion model has been shown to give satisfactory predictions of the combustion of wood volatiles above the bed of a semi-pilot-scale FBC.

REFERENCE

1. Lau, I. T. and Friedrich, F. D., Influence of fuel properties on fluidized bed combustion, *AIChE symposium series*, **84**(262), 89-101 (1988).
2. Felice, R. D., Coppola, G., Rapagna, S., and Jand, N., Modeling of biomass devolatilization in a fluidized bed reactor, *The Canadian J. of Chem. Eng.*, **77**, 325-332 (1999).
3. Jacobs, J. P., The future of fluidized-bed combustion, *Chem. Eng. Science*, **54**(22), 5559-5567 (1999).
4. Ho, T. C., Ku, P., and Hopper, J. R., Kinetic study of biological sludge incineration in a fluidized bed, *AiChE Symposium series*, **84**(263), 126-133 (1988).
5. Fiorentino, M., Marzocchella, A. and Salatino, P., Segregation of fuel particles and volatile mater during devolatilization in a fluidized bed reactor, *Chem. Eng. Science*, **52**(12), 1893-1908, (1997).
6. Ogada, T. and Werther, J., Combustion characteristics of wed sludge in a fluidized bed, *Fuel*, **75**(5), 617-625, (1996).
7. Park, D., Levenspiel, O., and Fitzgerald, T. J., *72nd Ann AIChE Meet*, San Francisco (1979).
8. Park, D., Levenspiel, O., and Fitzgerald, T. J., Plume model for large particle fluidized-bed combustor, *Fuel*, **60**(2), 295-306 (1981).
9. Park, D., Levenspiel, O. and Fitzgerald, T. J., A comparison of the plume model with currently used models of atomoshperic fluidized bed combustion, *Chem Eng Sci.*, **35**(1-2), 295-301 (1980).
10. Rajan, R. R. and Wen, C. Y., A comprehensive model for fluidized bed combustors, *AIChE J.*, **26**, 642-655 (1980).
11. Baron, R. E., Hodges, J. L., and Sarofim, A. F., A bubbling fluidization modeling using kinetic theory of granular flow, *AIChE Symp Ser* **176**(74), 120-125 (1978).
12. Borghi, G., Srofim, A. F., and Beer, J. M., *70th Ann AIChE Meet*, New York, (1977).
13. Jung, K. and Stanmore, B. R., Fluidized bed combustion of wet brown coal, *Feul*, **59**(1), 74-80 (1980).
14. Winter, F., Prah, M. E., and Hofbauer, H., Temperature in a fuel particle burning in a fluidized bed; the effect of drying, devolatilization and char combustion, *Combustion and Flame*, **108**, 302-314 (1997).
15. Atimtay, A., in Grace, J. R. and Matse, J. M., A evaluation of models for fluidized-bed reactors, Fluidization, 159-166, Plenum Press, New York, (1980).
16. Andrei, M. A., Srofim, A. F., and Beer, J. M., 86th Nat meet AIChE, Houston, Texas, Paper No. F, Session 57 (1979).
17. Phillai, K. K., A schematic for coal devolatilization and combustion, *J Inst Energy*, **54**, 142-150 (1981).
18. Sriramulu, S., Sane, S., Agarwal, P. and Mathews, T., Mathematical modeling of fluidized bed combustor; 1. combustion of carbon in bubbling bed, *Fuel*, **75**(12), pp.1351-1362, (1996).
19. Kunii, D. Levenspiel, O., Fluidization engineering. John Wiley & Sons Inc. London.
20. J. F. Davidson and D. Harrison, "Fluidized particle," Cambridge University Press, (1963).
21. Lim, K. S., Gururajan, V. S., and Agarwal,

P. K., Mixing of homogeneous solids in bubbling fluidized bed; theoretical modeling and experimental investigation using digital image analysis, *Chem. Eng. Sci.*, **48**(12), 2251-2265(1993).

22. La Nauze, R. D. and Jung, K., 19th Symp (Int) Combustion, Combustion Institution, Pittsburgh, Pennsylvania, 1087-1092 (1982).
23. Molerus, A. Burschka and S. Dietz, Particle migration at solid surfaces and heat transfer in bubbling flux beds, *Chem Eng Sci*, **50**(5), 879-885 (1995).
24. Smith, I. W., 19th Symp (Int) Combustion, Combustion Institute, Pittsburgh, Pennsylvania, 1045-1065 (1982).
25. Yu, Y. H., Kim, S. D., Lee J. M., and Lee, K. H., Kinetic studies of dehydration, pyrolysis and combustion of paper sludge, *Energy*, **27**, 457-469 (2002).
26. Blasi, C. D., Heat, momentum and mass transport through a shrinking biomass particle exposed to thermal radiation, *Chem Eng Sci.*, **51**(7), pp. 1121-1132 (1996).